

Cancellation of infrared divergences in bino-like theories of dark matter at finite temperature

Pritam Sen

based on arXiv : 1812.04247 (E.P.J. C79 (2019) no.6, 532) and
arXiv : 1812.06468 (Submitted)

with D. Indumathi (IMSc) and Debajyoti Choudhury (DU)

Presented at [WHEPP XVI 2019, IIT Guwahati](#)

6 th December, 2019



Introduction

- The existence of Dark Matter (DM) is widely accepted today to explain a multitude of astronomical and cosmological observations.
- It is popularly believed, that the DM particles are thermally produced in early universe.
- At high temperature a typical DM can stay in equilibrium with SM sector via processes like,

$$\chi + \bar{\chi} \leftrightarrow \mathcal{F}_{SM} + \overline{\mathcal{F}}_{SM} , \quad \text{and} \quad \chi + \mathcal{F}_{SM} \leftrightarrow \chi + \mathcal{F}_{SM}$$

- In this age of precision cosmology, the DM contribution to the energy budget of the universe is being measured with high accuracy by WMAP and PLANCK.



Introduction

- This relic density turns out to be of correct order, according to “WIMP paradigm” for a wide range of masses of DM.
- But, only an order of magnitude estimation is no longer acceptable at today’s date of precision cosmology.
- Both, the higher order corrections and the effects of non-zero temperature need to be considered.
- Initial efforts to include thermal corrections to relevant processes was made by M. Beneke et al. (JHEP 1410 (2014) 45), where it was shown the Infrared (IR) divergences to cancel out to NLO in collision processes.
- Here, we provide an all order proof of IR divergence cancellation for relevant theories, which is not only important for a prediction of correct relic abundance, but also for the consistency/possible existence of related DM particles.



A simplified theory of bino-like dark matter

- The Lagrangian relevant to this model is,

$$\mathcal{L} = -\frac{1}{4}F_{\mu\nu}F^{\mu\nu} + \bar{f} (i\not{D} - m_f) f + \frac{1}{2}\bar{\chi} (i\not{D} - m_\chi) \chi \\ + (D^\mu\phi)^\dagger (D_\mu\phi) - m_\phi^2\phi^\dagger\phi + (\lambda\bar{\chi}P_L f^-\phi^+ + \text{h.c.})$$

where, $f = (f^0, f^-)^T$ is a left-handed fermion doublet

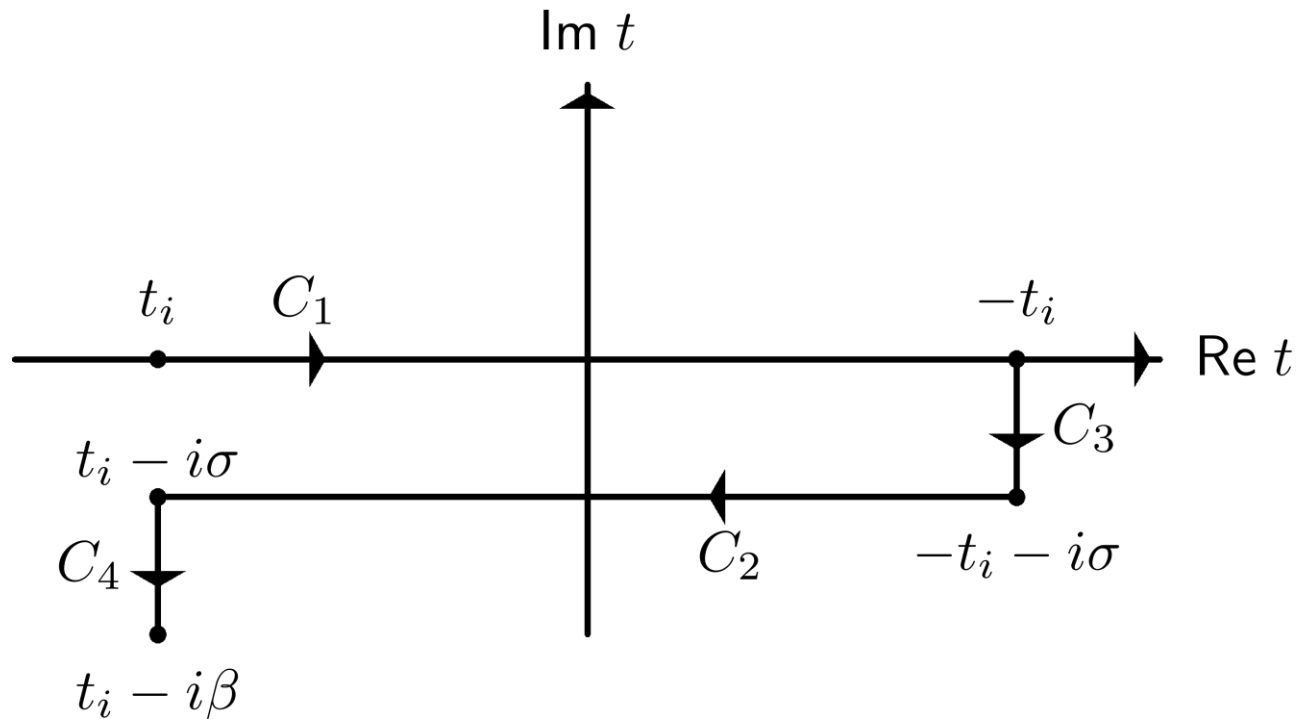
$\phi = (\phi^+, \phi^0)^T$ an additional scalar doublet

and, χ is a $SU(2) \times U(1)$ singlet Majorana Fermion.

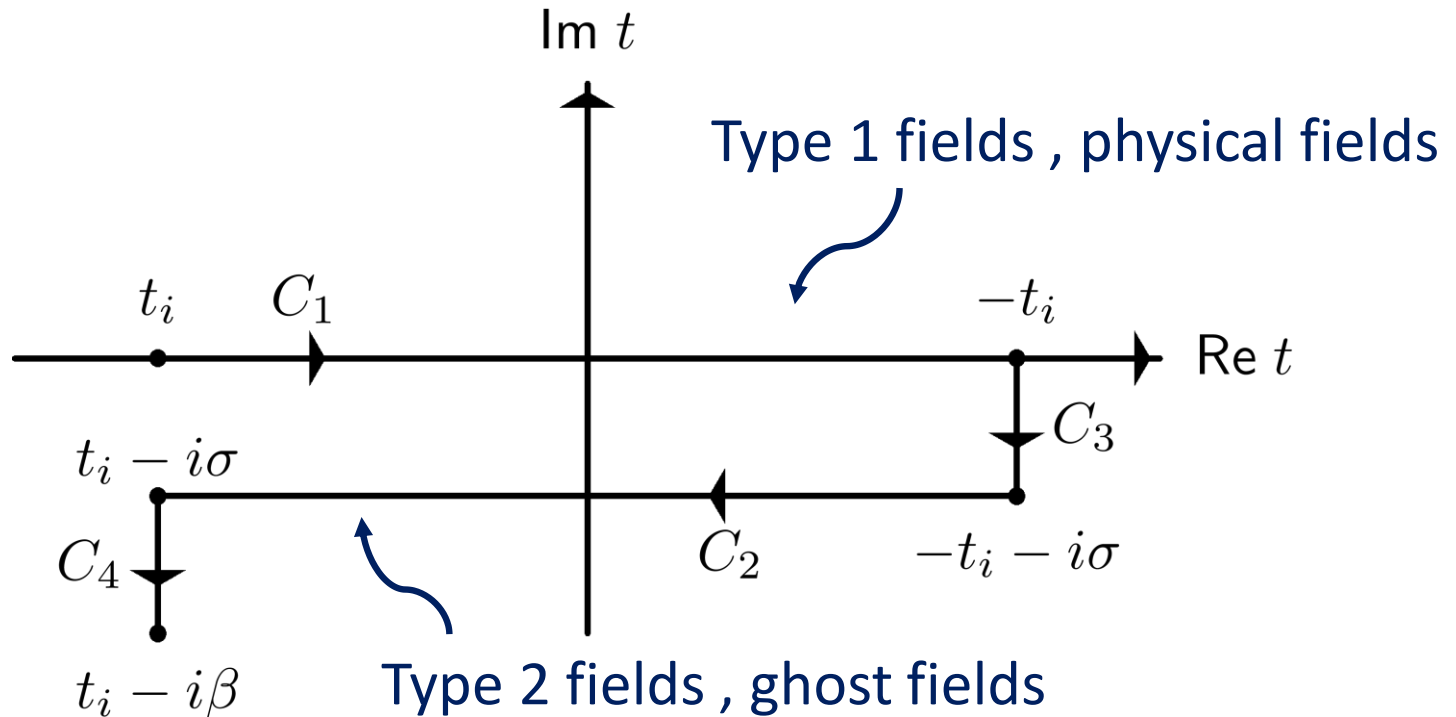
- We will assume bino to be a TeV scale DM, so-that freeze-out occurs after Electro-Weak phase transition.



Real time formulation of thermal field theory



Real time formulation of thermal field theory



This field doubling also results in extra thermal type of vertices, where all the field at a given vertex **must be** of the same thermal type.



Thermal Feynman rules

$$i\mathcal{D}_{\mu\nu}^{t_a t_b}(k) = -g_{\mu\nu} i\mathcal{D}^{t_a t_b}(k) ,$$

$$= \begin{pmatrix} \Delta(k) & 0 \\ 0 & \Delta^*(k) \end{pmatrix} + 2\pi\delta(k^2)N(|k^0|) \begin{pmatrix} 1 & e^{|k^0|/(2T)} \\ e^{|k^0|/(2T)} & 1 \end{pmatrix}$$

Where, $\Delta(k) = i/(k^2 + i\epsilon)$ and $t_a, t_b (= 1, 2)$ are thermal field type

$$i\mathcal{S}_{\text{fermion}}^{t_a t_b}(p, m) = \begin{pmatrix} S & 0 \\ 0 & S^* \end{pmatrix} - 2\pi S' \delta(p^2 - m^2) N_f(|p^0|) \begin{pmatrix} 1 & \epsilon(p_0) e^{|p^0|/(2T)} \\ -\epsilon(p_0) e^{|p^0|/(2T)} & 1 \end{pmatrix}$$

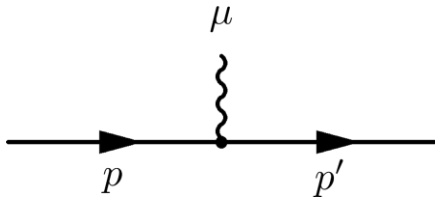
Where, $S = i/(\not{p} - m + i\epsilon)$, and $S' = (\not{p} + m)$

$$i\mathcal{S}_{\text{scalar}}^{t_a t_b}(p, m) = \begin{pmatrix} \Delta(p) & 0 \\ 0 & \Delta^*(p) \end{pmatrix} + 2\pi\delta(p^2 - m^2)N(|p^0|) \begin{pmatrix} 1 & e^{|p^0|/(2T)} \\ e^{|p^0|/(2T)} & 1 \end{pmatrix}$$

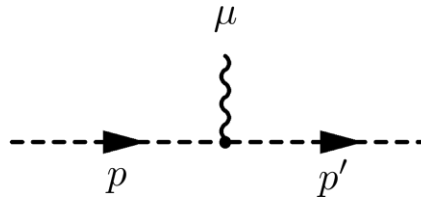
Where, $\Delta(p) = i/(p^2 - m^2 + i\epsilon)$



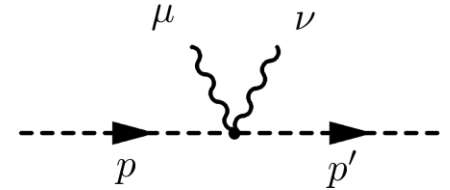
Thermal Feynman rules



$$(-ie\gamma_\mu)(-1)^{t_\mu+1}$$



$$[-ie(p_\mu + p'_\mu)](-1)^{t_\mu+1}$$



$$[+2ie^2 g_{\mu\nu}](-1)^{t_\mu+1}$$

For Fermions

$$N_f(|p^0|) \equiv \frac{1}{\exp\{|p^0|/T\} + 1}$$

$$\xrightarrow{p^0 \rightarrow 0} \frac{1}{2}$$

For Scalars

$$N(|k^0|) \equiv \frac{1}{\exp\{|k^0|/T\} - 1}$$

$$\xrightarrow{k^0 \rightarrow 0} \frac{T}{|k^0|} \longrightarrow \text{Divergence Worsens}$$

$$i\mathcal{D}^{ab}(k) \sim \left[\frac{i}{k^2 + i\epsilon} \delta^{ab} \pm \underbrace{2\pi \delta(k^2) N(|k^0|) D_T^{ab}} \right]$$

Linear Divergence



IR behaviour of scalar QED

- To separate out, IR finite and IR divergent parts we rearrange the polarisation sum of photon propagator into two parts using the technique of Grammar and Yennie .

For Virtual Photons :- (PRD 8, 4332 (1973))

$$\begin{aligned} -i \frac{g_{\mu\nu}}{k^2 + i\epsilon} &= \frac{-i}{k^2 + i\epsilon} [(g_{\mu\nu} - b_k(p_f, p_i)k_\mu k_\nu) + (b_k(p_f, p_i)k_\mu k_\nu)] , \\ &\equiv \frac{-i}{k^2 + i\epsilon} [G_{\mu\nu} + K_{\mu\nu}] \end{aligned}$$

Where,

$$b_k(p_f, p_i) = \frac{1}{2} \left[\frac{(2p_f - k) \cdot (2p_i - k)}{((p_f - k)^2 - m^2)((p_i - k)^2 - m^2)} + (k \leftrightarrow -k) \right]$$



IR behaviour of scalar QED

For Real Photons :-

By writing the polarization sum, $\sum_{\text{pol}} \epsilon_{\mu}^*(k) \epsilon_{\nu}(k) = -g_{\mu\nu}$

$$\text{As, } g_{\mu\nu} = \left\{ \left[g_{\mu\nu} - \tilde{b}_k(p_f, p_i) k_{\mu} k_{\nu} \right] + \left[\tilde{b}_k(p_f, p_i) k_{\mu} k_{\nu} \right] \right\} ,$$
$$\equiv \left\{ \left[\tilde{G}_{\mu\nu} \right] + \left[\tilde{K}_{\mu\nu} \right] \right\}$$

$$\text{Where, } \tilde{b}_k(p_f, p_i) = b_k(p_f, p_i) \Big|_{k^2=0} = \frac{p_f \cdot p_i}{k \cdot p_f k \cdot p_i}$$

Henceforth, we will talk in terms of K (\tilde{K}) and G (\tilde{G}) photons only.



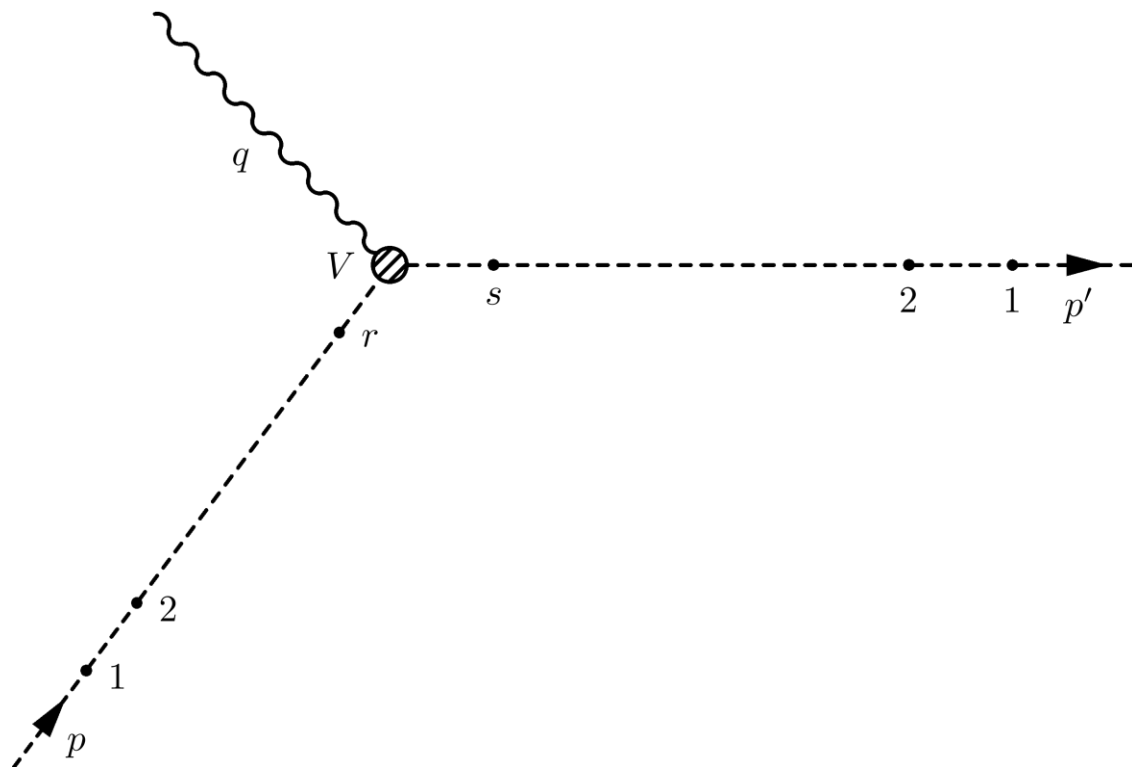
IR behaviour of scalar QED

- We will insert these K and G photons to a generic n-photon graphs (where, $r+s = n$) to analyze the structure of a higher order graph.

- Where, Photons carry away momenta l_q at vertex q on p - leg and momenta t_q on the p' - leg.

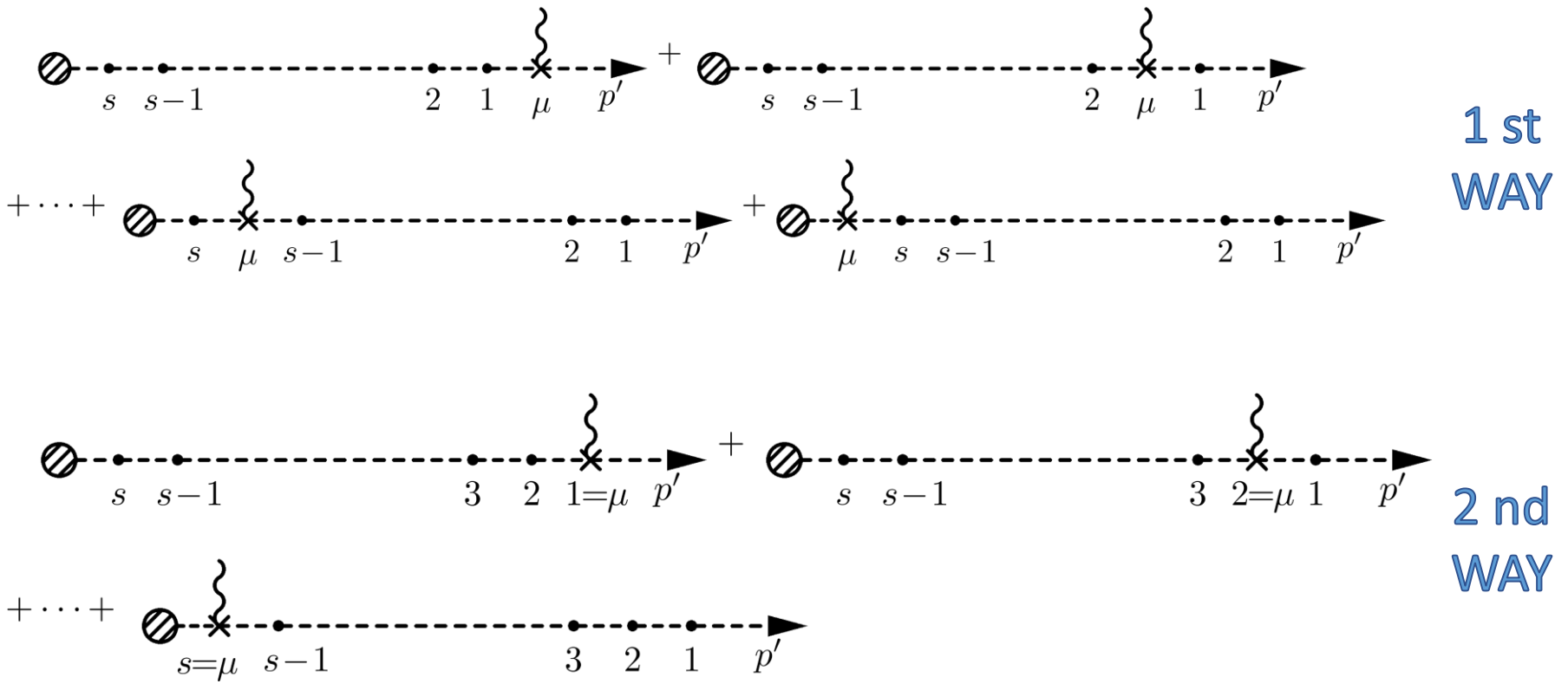
- And with notation,

$$i\mathcal{S}^{t_a t_b}(p' + \sum_{i=1}^q l_i, m) \equiv iS_{p'+\sum_q}^{ab}$$



Virtual K -photon calculations (p, p' insertion)

- Now because of the availability of additional type of vertices, the new (n+1) th K photon can add to lower order diagrams in two ways,



Virtual K -photon calculations (p, p' insertion)

- To ease out the calculation we define circled vertex as,

$$\begin{aligned}
 & \text{Diagram 1} - \text{Diagram 2} \\
 & \text{Diagram 1: } s \text{ --- } s-1 \text{ --- } q \text{ (x)} \text{ --- } q-1 \text{ --- } 2 \text{ --- } 1 \text{ --- } p' \\
 & \text{Diagram 2: } s \text{ --- } s-1 \text{ --- } q=\mu \text{ (x)} \text{ --- } q-1 \text{ --- } 2 \text{ --- } 1 \text{ --- } p' \\
 & \text{Diagram 3: } s \text{ --- } s-1 \text{ --- } q \text{ (O)} \text{ --- } q-1 \text{ --- } 2 \text{ --- } 1 \text{ --- } p'
 \end{aligned}$$

The contribution is difference of two terms,

$$\begin{aligned}
 \mathcal{M}_{n+1}^{q\mu, \text{tot}} = e^{s+1} (-1)^{(\sum_{i=1}^s t_i) + s} \dots & \left[S_{p'+\sum_{q-1}}^{q-1, q} \delta_{t_\mu, t_q} (2p' + 2\Sigma_{q-1} + l_q)_{\mu_q} \right. \\
 & \left. - S_{p'+\sum_{q-1} + k}^{q-1, q} \delta_{t_\mu, t_{q-1}} (2p' + 2\Sigma_{q-1} + 2k + l_q)_{\mu_q} \right] S_{p'+\sum_q + k}^{q, q+1} \dots
 \end{aligned}$$

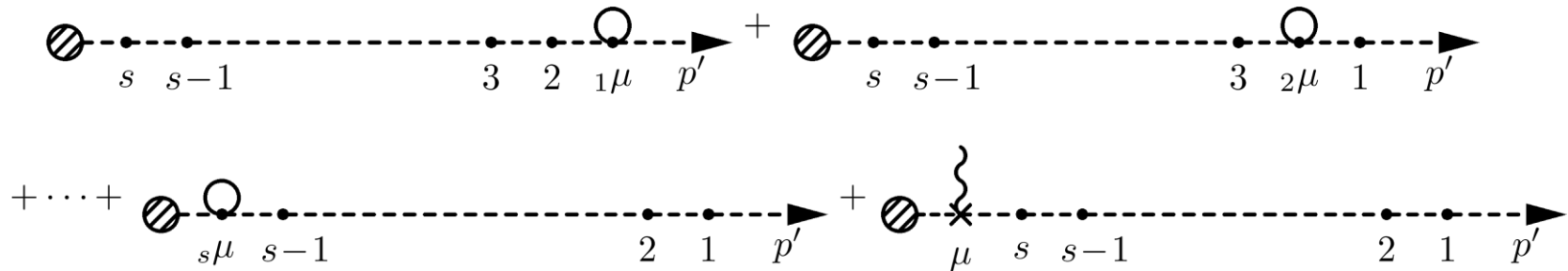
Where we have used Feynman's Identity for thermal field theory,

$$S_{p'+\Sigma_q}^{q\mu} [(2p' + 2\Sigma_q + k) \cdot k] S_{p'+\Sigma_q + k}^{\mu, q+1} = i(-1)^{t_\mu + 1} \left[S_{p'+\Sigma_q}^{q, q+1} \delta_{t_\mu, t_{q+1}} - S_{p'+\Sigma_q + k}^{q, q+1} \delta_{t_\mu, t_q} \right]$$



Virtual K -photon calculations (p, p' insertion)

- Now combining all of these Virtual K photon contributions on p' leg,

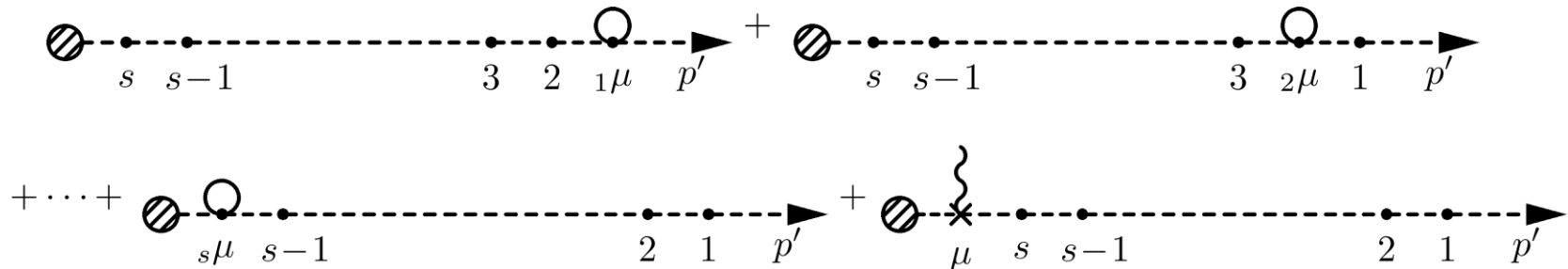


$$\begin{aligned}
 \mathcal{M}_{n+1}^{\mu, p', s} \propto & \left\{ 0 + \delta_{t_\mu, t_1} (2p' + l_1)_{\mu_1} S_{p'+\sum_1+k}^{t_1, t_2} (2p' + 2\Sigma_1 + 2k + l_2)_{\mu_2} \cdots (V) \cdots \right\} \\
 & + \left\{ (2p' + l_1)_{\mu_1} \left[S_{p'+\sum_1}^{t_1, t_2} \delta_{t_\mu, t_2} (2p' + 2\Sigma_1 + l_2)_{\mu_2} \right. \right. \\
 & \left. \left. - S_{p'+\sum_1+k}^{t_1, t_2} \delta_{t_\mu, t_1} (2p' + 2\Sigma_1 + 2k + l_2)_{\mu_2} \right] \cdots (V) \cdots \right\} \\
 & + \left\{ \cdots \right\} \\
 & + \left\{ (2p' + l_1)_{\mu_1} S_{p'+\sum_1}^{t_1, t_2} \cdots \left[S_{p'+\sum_{s-1}}^{t_{s-1}, t_s} \delta_{t_\mu, t_s} (2p' + 2\Sigma_{s-1} + l_s)_{\mu_s} \right. \right. \\
 & \left. \left. - S_{p'+\sum_{s-1}+k}^{t_{s-1}, t_s} \delta_{t_\mu, t_{s-1}} (2p' + 2\Sigma_{s-1} + 2k + l_s)_{\mu_s} \right] \cdots (V) \cdots \right\} ,
 \end{aligned}$$



Virtual K -photon calculations (p, p' insertion)

- Now combining all of these Virtual K photon contributions on p' leg,



$$\mathcal{M}_{n+1}^{\mu, p', s} \propto \{0 + M_1\} + \{M_2 - M_1\} + \{\dots\} + \{M_s - M_{s-1}\}$$

$$\begin{aligned} \mathcal{M}_{n+1}^{\mu, p', s+1} &\propto (2p' + l_1)_{\mu_1} S_{p'+\sum_1}^{t_1, t_2} \dots \left[S_{p'+\sum_s}^{t_s, t_V} \delta_{t_\mu, t_V} - S_{p'+\sum_s+k}^{t_s, t_V} \delta_{t_\mu, t_s} \right] (V) \dots, \\ &= \{M_{s+1} - M_s\} \end{aligned}$$



Virtual K -photon calculations (p, p' insertion)

- After combining these contributions we get,

$$\mathcal{M}_{n+1}^{\mu, p', tot} \propto (2p' + l_1)_{\mu_1} S_{p'+\Sigma_1}^{t_1, t_2} \cdots S_{p'+\Sigma_s}^{t_s, t_V} [\delta_{t_\mu, t_V}] (V) \cdots$$

- Following a similar procedure for p leg we get,

$$\mathcal{M}_{n+1}^{p' p, K\gamma} = -ie^2 \int \frac{d^4 k}{(2\pi)^4} \delta_{t_\mu, t_V} \delta_{t_\nu, t_V} b_k(p', p) D^{t_\mu, t_\nu}(k) \times \mathcal{M}_n$$

Thermal
Dependence

- We can follow the same procedure when both insertions of K photon are on p or p' leg.
- This cases are certainly, the most difficult ones as the number of relevant diagrams proliferate.
- We group those diagrams in sets namely, Set I , II , III and IV



Virtual K -photon calculations (p', p' insertion)

$$\begin{aligned}
 & \left[\begin{array}{c} \text{Diagram 1} \\ \text{Diagram 2} \end{array} + \dots + \right. \\
 & \left. + \left[\begin{array}{c} \text{Diagram 3} \\ \text{Diagram 4} \end{array} \right] + \left[\begin{array}{c} \text{Diagram 5} \\ \text{Diagram 6} \end{array} \right] + \dots + \left[\begin{array}{c} \text{Diagram 7} \end{array} \right]
 \end{aligned}$$

The diagrams in Set I are represented as follows:

- Diagram 1: A dashed line with a circled cross at the left end. Two vertices are marked with circles. The first vertex is labeled $s\nu$ and the second is $s-1$. The line ends in an arrow labeled p' .
- Diagram 2: Similar to Diagram 1, but the first vertex is labeled 2 and the second is 1μ .
- Diagram 3: Similar to Diagram 1, but the first vertex is labeled $s\nu$ and the second is $s-1\mu$.
- Diagram 4: Similar to Diagram 1, but the first vertex is labeled s and the second is $s-1\mu$.
- Diagram 5: Similar to Diagram 1, but the first vertex is labeled 2 and the second is 1μ .
- Diagram 6: Similar to Diagram 1, but the first vertex is labeled s and the second is $s-1$.
- Diagram 7: Similar to Diagram 1, but the first vertex is labeled 2ν and the second is 1μ .

Set I

$$\begin{array}{c} \text{Diagram 1} \\ \text{Diagram 2} \\ \dots \\ \text{Diagram 3} \end{array} + \dots + \begin{array}{c} \text{Diagram 4} \end{array}$$

The diagrams in Set II are represented as follows:

- Diagram 1: A dashed line with a circled cross at the left end. A vertex is marked with a cross labeled ν . Two vertices are marked with circles. The first vertex is labeled s and the second is $s-1$. The line ends in an arrow labeled p' .
- Diagram 2: Similar to Diagram 1, but the first vertex is labeled 2 and the second is 1μ .
- Diagram 3: Similar to Diagram 1, but the first vertex is labeled ν and the second is $s\mu$.

Set II

$$\begin{array}{c} \text{Diagram 1} \\ \text{Diagram 2} \\ \dots \\ \text{Diagram 3} \end{array} + \dots + \begin{array}{c} \text{Diagram 4} \end{array}$$

The diagrams in Set III are represented as follows:

- Diagram 1: A dashed line with a circled cross at the left end. Two vertices are marked with crosses. The first vertex is labeled $s=\nu$ and the second is μ . Two vertices are marked with circles. The first vertex is labeled $s-1$ and the second is 1 . The line ends in an arrow labeled p' .
- Diagram 2: Similar to Diagram 1, but the first vertex is labeled s and the second is $s-1=\nu$.
- Diagram 3: Similar to Diagram 1, but the first vertex is labeled s and the second is $s-1$.

Set III

$$\begin{array}{c} \text{Diagram 1} \\ \text{Diagram 2} \\ \dots \\ \text{Diagram 3} \end{array} + \dots + \begin{array}{c} \text{Diagram 4} \end{array}$$

The diagrams in Set IV are represented as follows:

- Diagram 1: A dashed line with a circled cross at the left end. Two vertices are marked with circles. The first vertex is labeled $\nu\mu$ and the second is s . Two vertices are marked with circles. The first vertex is labeled $s-1$ and the second is 1 . The line ends in an arrow labeled p' .
- Diagram 2: Similar to Diagram 1, but the first vertex is labeled s and the second is $\nu\mu$.
- Diagram 3: Similar to Diagram 1, but the first vertex is labeled s and the second is $s-1$.

Set IV



Schematic of K photon insertion p',p' leg

Linear in k with
 k dependence in denominator

Linear in k with no
 k dependence in denominator

$$\mathcal{M}_{n+1} \propto \mathcal{M}_n + \mathcal{O}_d(k) + \mathcal{O}(k) + \mathcal{O}(k^2)$$

Quadratic in
 k



Schematic of K photon insertion p',p' leg

Linear in k with
 k dependence in denominator

Linear in k with no
 k dependence in denominator

$$\mathcal{M}_{n+1} \propto \mathcal{M}_n + \cancel{\mathcal{O}_d(k)} + \cancel{\mathcal{O}(k)} + \cancel{\mathcal{O}(k^2)}$$

odd under integral
Hence vanishes

Quadratic in k

Exactly Cancels

+ Seagull

+ Tadpole

Leaving us with
exact
factorisation
leading to
resummation



Virtual K -photon calculations (p', p' insertion)

- After combining these contributions and symmetrizing on both leg we get,

$$\mathcal{M}_{n+1}^{p'p',K\gamma} = +ie^2 \frac{1}{2} \int \frac{d^4k}{(2\pi)^4} \delta_{t_\mu,t_1} \delta_{t_\nu,t_1} b_k(p',p') D^{t_\mu,t_\nu}(k) \mathcal{M}_n ,$$

$$\mathcal{M}_{n+1}^{pp,K\gamma} = +ie^2 \frac{1}{2} \int \frac{d^4k}{(2\pi)^4} \delta_{t_\mu,t_1} \delta_{t_\nu,t_1} b_k(p,p) D^{t_\mu,t_\nu}(k) \mathcal{M}_n$$



Virtual K -photon calculations

- Hence, the total Virtual K-photon contribution becomes,

$$\begin{aligned}\mathcal{M}_{n+1}^{K\gamma, \text{tot}} &= \frac{ie^2}{2} \int \frac{d^4k}{(2\pi)^4} \left\{ \delta_{t_\mu, t_1} \delta_{t_\nu, t_1} D^{t_\mu, t_\nu}(k) [b_k(p', p') + b_k(p, p)] \right. \\ &\quad \left. + \delta_{t_\mu, t_V} \delta_{t_\nu, t_V} D^{t_\mu, t_\nu}(k) [-2b_k(p', p)] \right\} \mathcal{M}_n, \\ &\equiv [B] \mathcal{M}_n\end{aligned}$$

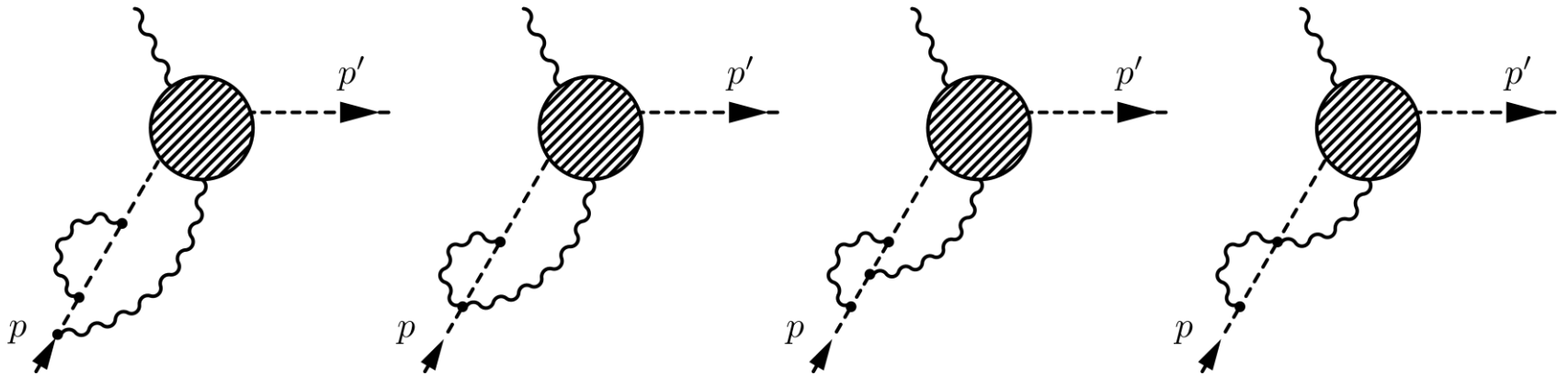
- Where,

$$\begin{aligned}B &= \frac{ie^2}{2} \int \frac{d^4k}{(2\pi)^4} D^{11}(k) [b_k(p', p') - 2b_k(p', p) + b_k(p, p)] , \\ &\equiv \frac{ie^2}{2} \int \frac{d^4k}{(2\pi)^4} D^{11}(k) [J^2(k)]\end{aligned}$$



Dissallowed diagrams

- All the disallowed diagrams which are allowed in higher order gives zero contribution.



Virtual G -photon calculations

- This is the most difficult calculation , as these diagrams also have sub-leading divergences due to number operator.

- But b simplifies to, $b_k^{T \neq 0}(p_f, p_i) = \frac{p_f \cdot p_i}{p_f \cdot k p_i \cdot k}$.

$$\mathcal{M}_{n+1}^{G\gamma} \sim \int d^4k \left[\frac{i}{k^2 + i\epsilon} \delta_{t_\mu, t_\nu} \pm 2\pi\delta(k^2)N(|k|)D_T^{t_\mu, t_\nu} \right] [g^{\mu\nu} - b_k k^\mu k^\nu] [\text{scalar}]_{\mu\nu}$$

- After removing the μ and ν contribution from scalar part

$$\mathcal{M}_{n+1}^{G\gamma} \sim \int d^4k \left[\frac{i}{k^2 + i\epsilon} \delta_{t_\mu, t_\nu} \pm 2\pi\delta(k^2)N(|k|)D_{t_\mu, t_\nu} \right] [0(p_f \cdot p_i) + 2(p_f + p_i) \cdot k] [\text{scalar}]_{\mu\psi}$$

- Where, $[\text{scalar}]_{\mu\psi} \sim [\mathcal{O}(1) + \mathcal{O}(k) + \mathcal{O}(k^2) + \dots]$

- The G photon contribution is shown to be IR finite.



Virtual photon factorisation and resummation

- After taking into account of all the particular ways in which a matrix element can arise, we are able to write,

$$\begin{aligned} \sum_{n=0}^{\infty} \frac{1}{n!} \mathcal{M}_n &= \sum_{n=0}^{\infty} \sum_{n_K=0}^n \frac{1}{n_K!} \frac{1}{n-n_K!} \mathcal{M}_{n_G, n_K} , \\ &= \sum_{n_K=0}^{\infty} \sum_{n_G=0}^{\infty} \frac{1}{n_K!} \frac{1}{n_G!} \mathcal{M}_{n_G, n_K} \end{aligned}$$

- And, $\mathcal{M}_{n_G, n_K} = (B)^{n_K} M_{n_G, 0} \equiv (B)^{n_K} M_{n_G}$

- Hence,
$$\sum_{n=0}^{\infty} \frac{1}{n!} \mathcal{M}_n = \sum_{n_K=0}^{\infty} \frac{(B)^{n_K}}{n_K!} \sum_{n_G=0}^{\infty} \frac{1}{n_G!} \mathcal{M}_{n_G} ,$$

Divergence \longrightarrow
$$= e^B \sum_{n_G=0}^{\infty} \frac{1}{n_G!} \mathcal{M}_{n_G}$$



Real photon emission and absorption

- Considering the rearranged polarization sum for real photons, and after realizing the fact that, real photons can **both be absorbed from and emitted to heat bath** at finite temperature, we get the cross section for real \tilde{K} photon as,

$$\left| \mathcal{M}_{n+1}^{\tilde{K}\gamma, \text{tot}} \right|^2 \propto -e^2 \left[\tilde{b}_k(p, p) - 2\tilde{b}_k(p', p) + \tilde{b}_k(p', p') \right] ,$$

$$\equiv -e^2 \tilde{J}^2(k)$$

- And For Real \tilde{G} Photon $\propto -\tilde{G}_{\mu\nu} \left| \mathcal{M}_{n_G}^{\mu\nu, \tilde{G}\gamma, \text{tot}} \right|^2$

- With, $\tilde{B}(x) = -e^2 \int \tilde{J}^2(k_k) d\phi_k \exp [\pm i k_k \cdot x]$

- And , $d\phi_i = \frac{d^4 k_i}{(2\pi)^4} 2\pi \delta(k_i^2) [\theta(k_i^0) + N(|k_i^0|)] ;$



Total cross-section for thermal scalar QED

- The total cross-section turns out to be,

$$d\sigma^{tot} = \int d^4x e^{(p+q-p')\cdot x} d\phi_{p'} \exp [B + B^*] \exp [\tilde{B}] \times \sum_{n_G=0}^{\infty} \frac{1}{n_G!}$$

$$\prod_{j=0}^{n_G} \times \int d\phi_j e^{\pm i k_j \cdot x} [-G_{\mu\nu} \mathcal{M}_{n_G}^{\dagger\mu} \mathcal{M}_{n_G}^{\nu}]$$

$$d\sigma^{tot} = \int d^4x e^{-i(p+q-p')\cdot x} d\phi_{p'} \exp [B + B^* + \tilde{B}] \sigma^{finite}(x)$$

- And, as,

$$(B + B^*) + \tilde{B} = e^2 \int d\phi_k [J(k)^2 [1 + 2N(|k^0|)] - \tilde{J}(k^2) [(1 + N(|k^0|)) e^{ik\cdot x} + N(|k^0|) e^{-ik\cdot x}]]$$

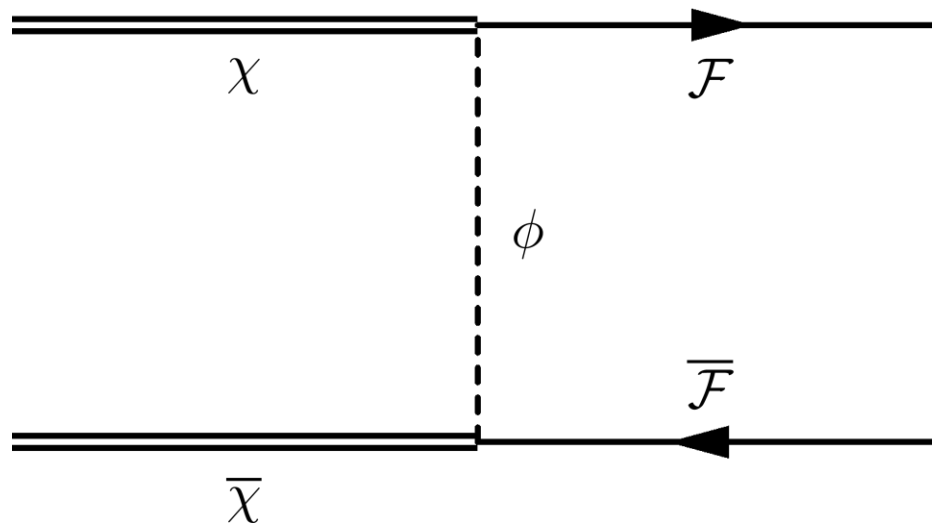
$$\xrightarrow{k \rightarrow 0} 0 + \mathcal{O}(k^2)$$

Hence, Thermal Scalar-QED Is free from IR divergence at all orders in perturbative theory.



Finally getting back to processes related to DM

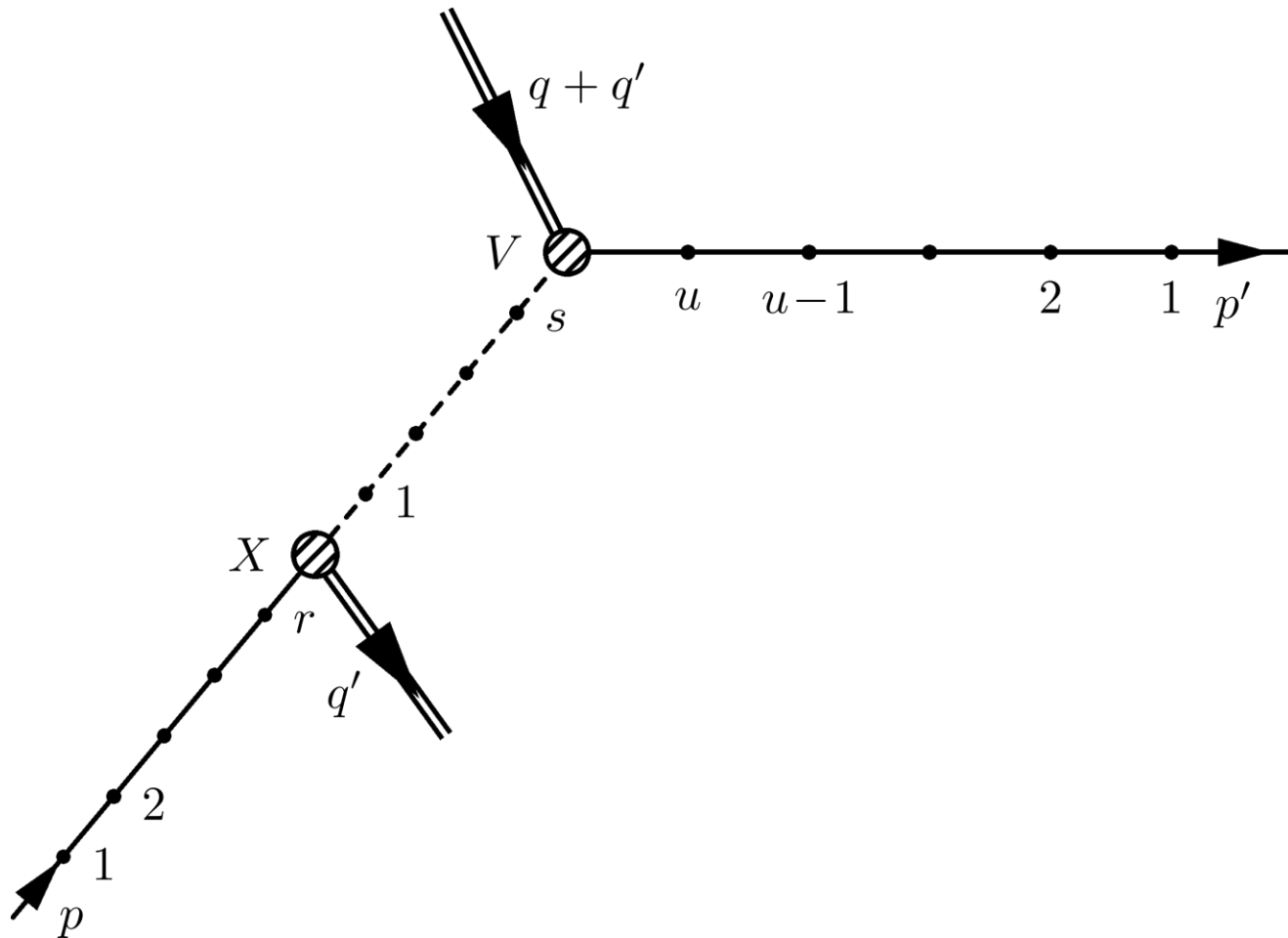
- A generic scattering process in this model of bino-like DM looks like,



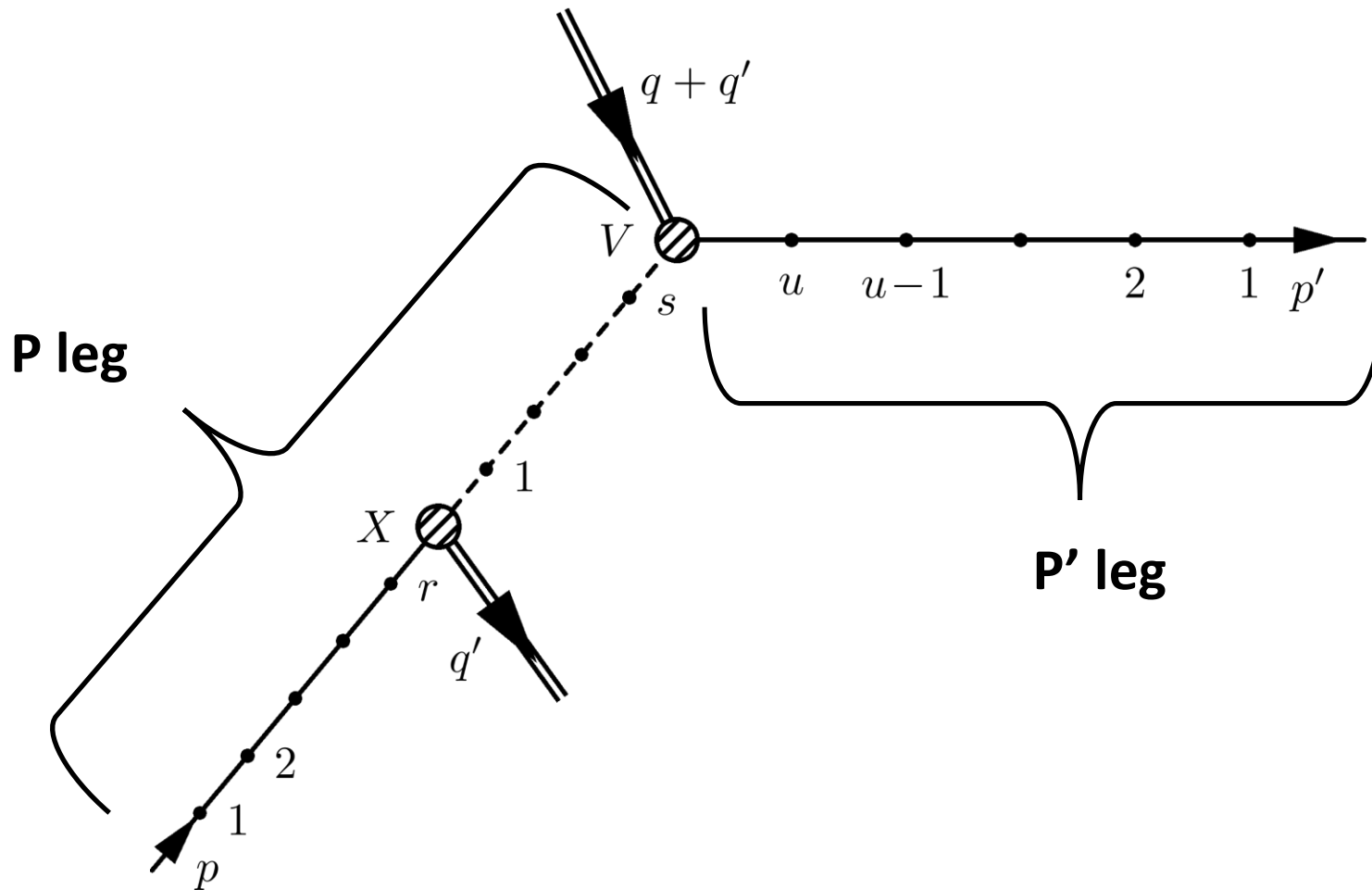
- To follow the above procedure we have to identify correctly the corresponding analogous p, p' leg for this process.



Identification of p, p' legs



Identification of p, p' legs



Virtual K photon calculation

- We can express N th matrix element generically as,

$$\mathcal{M}_n^{p_f, p_i} = C_u^{\text{fermion } p'} \times C_s^{\text{scalar}} \times C_r^{\text{fermion } p}$$

- Repeating a similar procedure as above we get,

For both the insertions on p' leg :-

$$\mathcal{M}_{n+1}^{p' p', K\gamma} = +ie^2 \int \frac{d^4 k}{(2\pi)^4} \delta_{t_\mu, t_1} \delta_{t_\nu, t_1} b_k(p', p') D^{t_\mu, t_\nu}(k) \mathcal{M}_n$$

For the insertions between p, p' leg :-

$$\mathcal{M}_{n+1}^{p', p} \sim C_{u+1}^{\text{fermion } p', \mu} \times C_{r+s+1}^{p, \nu}$$



Virtual K photon calculation

- Now, after some calculation we get,

$$C_{u+1}^{\text{fermion } p', \mu} \sim \bar{u}_{p'} \gamma_{\mu_1} S_{p'+\sum_1}^{t_1 t_2} \cdots (\text{no } k) \cdots S_{p'+\sum_s}^{t_s t_V} \delta_{t_\mu, t_V} \Gamma_V u_{q+q'}$$

- And,

$$C_{r+s+1}^{p, \nu} \sim \left[C_{s+1}^{\text{scalar}, \nu} \times C_r^{\text{fermion } p}(q_i) + C_s^{\text{scalar}}(q_i \rightarrow q_i + k) \times C_{r+1}^{\text{fermion } p, \nu} \right]$$

$$C_{s+r+1}^{p, \nu} \sim \left\{ \left[\delta_{t_\nu, t_V} S_{P+\sum_s}^{t_V, t_s} \cdots S_{P+\sum_1}^{t_2, t_1} (2P + l_1)_{\mu_1} S_P^{t_1, t_X} \right. \right. \\ \left. \left. - \delta_{t_\nu, t_X} S_{P+\sum_s+k}^{t_V, t_s} \cdots (2P + 2k + l_1)_{\mu_1} S_{P+k}^{t_1, t_X} \right] \times \left[\bar{u}_{q'} \Gamma_X S_{p+\sum_r}^{t_X, t_r} \gamma_r \cdots (\text{no } k) u_p \right] \right\} \\ + \left\{ \left[S_{P+\sum_s+k}^{t_V, t_s} \cdots (2P + 2k + l_1)_{\mu_1} S_{P+k}^{t_1, t_X} \right] \times \left[\bar{u}_{q'} \Gamma_X S_{p+\sum_r}^{t_X, t_r} \delta_{t_\nu, t_X} \gamma_r \cdots (\text{no } k) u_p \right] \right\} \\ = \left[\delta_{t_\nu, t_V} S_{P+\sum_s}^{t_V, t_s} \cdots S_{P+\sum_1}^{t_2, t_1} (2P + l_1)_{\mu_1} S_P^{t_1, t_X} \right] \times \left\{ \bar{u}_{q'} \Gamma_X S_{p+\sum_r}^{t_X, t_r} \gamma_r \cdots (\text{no } k) u_p \right\}$$

cancellation



Virtual K photon calculation

- Hence, the total p', p contribution turns out to be,

$$\mathcal{M}_{n+1}^{p'p, K\gamma} = -ie^2 \int \frac{d^4k}{(2\pi)^4} \delta_{t_\mu, t_\nu} \delta_{t_\nu, t_\nu} b_k(p', p) D^{t_\mu, t_\nu}(k) \times \mathcal{M}_n$$

For the insertions between p, p leg :-

$$\mathcal{M}_{n+1}^{p,p} \sim \mathcal{C}_u^{\text{fermion } p'} \times \left[\mathcal{C}_s^{\text{scalar}} \times \mathcal{C}_{r+2}^{\text{fermion } p; \mu, \nu} + \mathcal{C}_{s+1}^{\text{scalar}; \mu} \times \mathcal{C}_{r+1}^{\text{fermion } p; \nu} + \mathcal{C}_{s+2}^{\text{scalar}; \mu, \nu} \times \mathcal{C}_r^{\text{fermion } p} \right]$$

Now we can show that, $\mathcal{C}_{r+2}^{\text{fermion } p; \mu, \nu} = 0$;

Hence, $\mathcal{C}_s^{\text{scalar}} \times \mathcal{C}_{r+2}^{\text{fermion } p; \mu, \nu} = 0$



Schematics of the result for pp leg K photon

$$\begin{aligned}
 C_{s+2}^{\text{scalar};\mu\nu} &\sim \left[C_{s+2}^{\text{scalar};\mu;\nu,I} + C_{s+2}^{\text{scalar};\mu;\nu,II} + C_{s+2}^{\text{scalar};\mu;\nu,III} + C_{s+2}^{\text{scalar};\mu;\nu,IV} \right] \\
 &\equiv \left\{ - \sum_{q=1}^s C_1^{q;SS} - C_2^{SS} + C_3^{SS} \right\} \leftarrow k \text{ dependence} \\
 &\quad \uparrow \\
 &\quad \sim [\delta_{t_\mu, t_V} \delta_{t_\nu, t_V}]
 \end{aligned}$$

k dependence \rightarrow (pointing to the sum and C_3^{SS})



Schematics of the result for pp leg K photon

$$\begin{aligned}
 C_{s+2}^{\text{scalar};\mu\nu} &\sim \left[C_{s+2}^{\text{scalar};\mu;\nu,I} + C_{s+2}^{\text{scalar};\mu;\nu,II} + C_{s+2}^{\text{scalar};\mu;\nu,III} + C_{s+2}^{\text{scalar};\mu;\nu,IV} \right] \\
 &\equiv \left\{ - \sum_{q=1}^s C_1^{q;ss} - C_2^{ss} + C_3^{ss} \right\} \leftarrow k \text{ dependence} \\
 &\sim [\delta_{t_\mu, t_V} \delta_{t_\nu, t_V}]
 \end{aligned}$$

\nearrow k dependence \uparrow \nwarrow k dependence

And

$$\begin{aligned}
 C_{s+1}^{\text{scalar};\mu} \times C_{r+1}^{\text{fermion } p;\nu} &\sim C_{s+1}^{\text{scalar};\mu} \delta_{t_\nu, t_X} , \\
 &\equiv \left\{ \sum_{q=1}^s C_1^{q;sf} + C_2^{sf} - C_3^{sf} \right\} \leftarrow k \text{ dependence} \\
 &\sim [\delta_{t_\mu, t_X} \delta_{t_\nu, t_X}]
 \end{aligned}$$

\nearrow k dependence \uparrow \nwarrow k dependence



Schematics of the result for pp leg K photon

$$C_{s+2}^{\text{scalar};\mu\nu} \sim \left[C_{s+2}^{\text{scalar};\mu;\nu,I} + C_{s+2}^{\text{scalar};\mu;\nu,II} + C_{s+2}^{\text{scalar};\mu;\nu,III} + C_{s+2}^{\text{scalar};\mu;\nu,IV} \right]$$

$$\equiv \left\{ - \sum_{q=1}^s \cancel{C_1^{q;ss}} - \cancel{C_2^{ss}} + \cancel{C_3^{ss}} \right\} \quad k \text{ dependence}$$

$\sim [\delta_{t_\mu, t_V} \delta_{t_\nu, t_V}]$

Nontrivial cancellation
giving total contribution from pp leg to be ZERO

And

$$C_{s+1}^{\text{scalar};\mu} \times C_{r+1}^{\text{fermion } p;\nu} \sim C_{s+1}^{\text{scalar};\mu} \delta_{t_\nu, t_X} ,$$

$$\equiv \left\{ \sum_{q=1}^s \cancel{C_1^{q;sf}} + \cancel{C_2^{sf}} - \cancel{C_3^{sf}} \right\} \quad k \text{ dependence}$$

$\sim [\delta_{t_\mu, t_X} \delta_{t_\nu, t_X}]$



Virtual K -photon total contribution

- Hence, the total Virtual K-photon contribution again looks like,

$$\begin{aligned}\mathcal{M}_{n+1}^{K\gamma, \text{tot}} &= \frac{ie^2}{2} \int \frac{d^4k}{(2\pi)^4} \left\{ \delta_{t_\mu, t_1} \delta_{t_\nu, t_1} D^{t_\mu, t_\nu}(k) [b_k(p', p') + b_k(p, p)] \right. \\ &\quad \left. + \delta_{t_\mu, t_V} \delta_{t_\nu, t_V} D^{t_\mu, t_\nu}(k) [-2b_k(p', p)] \right\} \mathcal{M}_n, \\ &\equiv [B] \mathcal{M}_n\end{aligned}$$

- Where,

$$\begin{aligned}B &= \frac{ie^2}{2} \int \frac{d^4k}{(2\pi)^4} D^{11}(k) [b_k(p', p') - 2b_k(p', p) + b_k(p, p)] , \\ &\equiv \frac{ie^2}{2} \int \frac{d^4k}{(2\pi)^4} D^{11}(k) [J^2(k)]\end{aligned}$$



Virtual G -photon calculations

- G photons again turn out to be finite as earlier case.
- There can be some other possibilities for virtual G-photon insertion as,
 1. Virtual G photon insertion on skeletal graphs
 2. Including Seagull diagrams into the picture
 3. Scalar, and Fermions lines can be thermal.
 4. There could have been K photon vertices
 5. There could have been some real photon vertices
- All of the above-mentioned cases have been studied individually, and was found to give finite result.



Real photon emission and absorption

- Real photon emission and absorption in terms of the modified polarization sum gives a similar result as before.
- Real \tilde{K} photons were found to have divergence pieces, which were factorized neatly.
- The real \tilde{G} photon contributions were finite.



Total cross-section for thermal bino-like DM

- The total cross-section again turns out to be,

$$d\sigma^{tot} = \int d^4x e^{(p+q-p')\cdot x} d\phi_{p'} \exp [B + B^*] \exp [\tilde{B}] \times \sum_{n_G=0}^{\infty} \frac{1}{n_G!}$$

$$\prod_{j=0}^{n_G} \times \int d\phi_j e^{\pm i k_j \cdot x} [-G_{\mu\nu} \mathcal{M}_{n_G}^{\dagger\mu} \mathcal{M}_{n_G}^{\nu}]$$

$$d\sigma^{tot} = \int d^4x e^{-i(p+q-p')\cdot x} d\phi_{p'} \exp [B + B^* + \tilde{B}] \sigma^{finite}(x)$$

- And, as,

$$(B + B^*) + \tilde{B} = e^2 \int d\phi_k [J(k)^2 [1 + 2N(|k^0|)] - \tilde{J}(k^2) [(1 + N(|k^0|)) e^{ik\cdot x} + N(|k^0|) e^{-ik\cdot x}]]$$

$$\xrightarrow{k \rightarrow 0} 0 + \mathcal{O}(k^2)$$

Hence, Thermal theory of bino-like Dark Matter is free of IR divergence at all orders.



Summary and Conclusion

- Using the IR finiteness of a thermal theory of Charged scalars, and fermionic QED the bino-like theory of DM are found to be IR safe at all orders in perturbation theory.
- The seagull and tadpole diagrams were crucial to obtain a neat factorization leading to resummation.
- Both the emission to and absorption from heat bath was crucial for the IR divergence cancellation.
- The whole procedure does not depend on the exact interaction term in the Lagrangian, and hence can be easily applied to any theory of charged scalars and fermion.
- Above, the IR cut-off the presence of heat bath becomes discernible.
- The IR finiteness of DM is a generic requirement, absence of which has dire implications in the cosmology.





Thank You.

